



Luteolin Could Improve Cognitive Dysfunction by Inhibiting Neuroinflammation

Zhao-Hui Yao¹ · Xiao-li Yao² · Yong Zhang³ · Shao-feng Zhang³ · Ji-chang Hu⁴

Received: 3 October 2017 / Revised: 15 January 2018 / Accepted: 20 January 2018 / Published online: 1 February 2018
© Springer Science+Business Media, LLC, part of Springer Nature 2018

Abstract

Neuroinflammation and oxidative stress play an important role in cognition deficit following chronic cerebral hypoperfusion (CCH). Luteolin, a natural flavonoid found in many plants, is known for a variety of pharmacological activities, such as its anti-inflammatory, anti-allergy, urate, anti-tumor, antibacterial, and antiviral effects. To assess whether luteolin could prevent CCH-induced cognitive dysfunction, through its anti-inflammatory and anti-oxidative-stress effects, we used enzyme-linked immunosorbent assays, enzyme activity assays, behavioral methods, immunohistochemistry, and electrophysiology to detect neuroinflammation and oxidative stress, cognition alterations, and long-term potential (LTP), in a bilateral common carotid arteries ligation (2VO) rat model. We demonstrated that CCH increased tumor necrosis factor α (TNF- α), interleukin 1 β (IL-1 β), interleukin 6 (IL-6), and malondialdehyde (MDA), and decreased superoxide dismutase (SOD) and glutathione peroxidase (GPx) levels. Further, it caused microglia over-activation and astrogliosis, learning and short-term memory dysfunction, and an LTP deficit. Luteolin treatment reversed CCH-induced changes. Specifically, luteolin prevented the increase of TNF- α and IL-1 β , IL-6, and MDA, improved the activity of SOD and GPx, inhibited microglia over-activation and astrogliosis (particularly in the hippocampus and cortex), and ameliorated learning and short-term memory dysfunction, and LTP deficit. Thus, our study suggested that luteolin could be a preferable anti-inflammatory agent to protect cognitive function and synaptic plasticity following CCH. Luteolin could also be putative therapeutic candidate for other inflammation-related brain diseases.

Keywords Chronic cerebral hypoperfusion · Cognition dysfunction · Neuroinflammation · Luteolin

Abbreviations

A β ₄₀	Amyloid β -protein 40	DAB	Diaminobenzidine
AP-1	Activating protein-1	ELISA	Enzyme-linked immunosorbent assay
BBB	Blood–brain barrier	fEPSPs	Field excitatory postsynaptic potential
BSA	Bovine serum albumin	GABA	γ -Aminobutyric acid
CCH	Chronic cerebral hypoperfusion	GAPDH	Glyceraldehyde 3-phosphate dehydrogenase
cDNA	Complementary DNA	GFAP	Glial fibrillary acidic protein
Con	Control group	GPx	Glutathione peroxidases
COX-2	Cyclooxygenase-2	HRP	Horseradish peroxidase
		HFS	High frequency stimulation
		IBA-1	Ionized calcium-binding adapter molecule 1
		IL-1 β	Interleukin 1 β
		IL-6	Interleukin 6
		IL-8	Interleukin-8
		LPS	Lipopolysaccharide
		I κ B- α	Kappa B-alpha
		iNOS	Inducible nitric oxide synthase
		KA	Kainic acid
		LTP	Long-term potentiation
		Lut	Luteolin treatment
		mAb	Mouse monoclonal antibody

✉ Zhao-Hui Yao
yaozhaohui2004@126.com

¹ Department of Geriatrics, Renmin Hospital of Wuhan University, #238 Jiefang Road, Wuhan 430060, China

² Department of Neurology, Central Hospital of Zhengzhou, #195 Tongbo Road, Zhengzhou, China

³ Department of Neurology, Renmin Hospital of Wuhan University, #238 Jiefang Road, Wuhan, China

⁴ Department of Pathology, Renmin Hospital of Wuhan University, #238 Jiefang Road, Wuhan, China

MAPK	Mitogen-activated protein kinase
MDA	Malondialdehyde
MWM	Morris water maze
NSFC	National Natural Science Foundation of China
NO	Nitric oxide
PP	Perforant path
NOR	Novel object recognition test
PPF	Paired-pulse facilitation
qRT-PCR	Quantitative real time polymerase chain reaction
SDS-PAGE	Sodium dodecyl sulfate polyacrylamide gel electrophoresis
SOD	Superoxide dismutase
TNF- α	Tumor necrosis factor α
TUNEL	Terminal deoxynucleotidyl transferase (TdT)-mediated dUTP nick end labelling
2VO	Bilateral common carotid arteries ligation
2VO + Lut	2VO operation and luteolin treatment

Introduction

Chronic cerebral hypoperfusion (CCH) occurs in many cognition-related diseases, such as vascular dementia, Alzheimer's disease, Parkinson disease dementia, etc. In these diseases, CCH played a major role in advancing the progress of diseases. A recent study also showed that CCH could independently exacerbate cognitive impairment during the pathogenesis of Parkinson's disease [1], which further illustrated the important role of CCH in cognitive dysfunction. Due to a long-term reduction in blood supply to brain, CCH-induced oxidative stress and inflammation can cause axon demyelination, glia over-activation, white matter lesions, blood–brain barrier (BBB) breakdown, and generation of endogenous toxic substances, such as oxygen free radical, amyloid beta protein (A β), and hyperphosphorylated tau proteins, which can impair cognition through varied mechanisms.

Following CCH, the generation of A β was accompanied by neuroinflammation with microglial or astroglial activation in the hippocampus or white matter, and white matter lesions [2]. Oxiracetam, a nootropic drug, improved neuron damage and white matter lesions, and inhibited astrocyte activation, thus, alleviating spatial learning and memory impairments, in a rat model of CCH [3]. Exposure to an enriched environment could also improve the cognition of patients with vascular dementia, which is characterized by reduced white matter disease-related inflammation and glial activation [4]. Further, huperzine could also improve chronic inflammation and cognitive decline in CCH rats [5]. These results suggested that neuroinflammation plays an important role in cognitive impairment caused by CCH; it may even be at the core of the progression of cognitive impairment. Thus, direct inhibition of inflammation could

yield a better therapeutic effect on cognition dysfunction after CCH. Thus, drugs or other methods that effectively treat anti-neuroinflammation, could also be therapeutically applied to treat cognitive impairment induced by CCH.

Luteolin (3',4',5,7-tetrahydroxyflavone), which is a member of the flavone subclass of flavonoids found in many plants [6], has many biological functions, including antioxidant, anti-mutagenic, anti-inflammatory, and anti-allergic activities [7–9]. A previous study demonstrated that luteolin significantly reduced lipopolysaccharide (LPS)-induced inflammation, through the inhibition of pro-inflammatory molecule expression and leukocyte infiltration [8, 9]. Further, luteolin also significantly reduced the levels of interleukin-8 (IL-8) and cyclooxygenase-2 (COX-2), and inducible nitric oxide synthase (iNOS) and nitric oxide (NO), which were induced by cytokines [10]. Luteolin also protected mice against severe acute pancreatitis and retinal pigment epithelial cells against oxidative stress by anti-inflammatory and antioxidant effects [11, 12]. Luteolin was also profoundly effective against neurological diseases. It protected the BBB from A β_{40} -induced damage, by inhibiting inflammation [13]. Luteolin could also attenuate kainic acid (KA)-induced neuronal death and microglial activation by effectively preventing hippocampal inflammation [14]. Further, it also prevented neuroinflammation following spinal cord injury by inhibiting COX-2 and iNOS [15]. Thus, luteolin had a strong anti-inflammatory effect. Since neuroinflammation plays a key role in cognitive impairment caused by CCH, we speculated that luteolin could also improve CCH-induced cognitive impairment. However, this has not been reported thus far.

Therefore, in the present study we investigated the effect of luteolin on neuroinflammation, oxidative stress, and impaired cognitive impairment and synaptic plasticity, which were caused by CCH. Our findings showed that luteolin decreased malondialdehyde (MDA), and inflammatory factors, such as TNF-1 α , IL-1 β , and IL-6, and enhanced the activity of superoxide dismutase (SOD) and glutathione peroxidase (GPx). It also reduced CCH-induced microglia over-activation and astrogliosis in the hippocampus and cortex, and ameliorated the effects of CCH on white matter, paired-pulse facilitation (PPF), long-term potentiation (LTP), spatial learning, and memory. Thus, our study suggested that luteolin could be a preferential anti-inflammatory agent that is used to protect cognition function and synaptic plasticity following CCH.

Methods and Materials

Antibodies and Chemicals

Mouse monoclonal antibody (mAb) β -actin to total β -actin and rabbit pAb against ionized calcium-binding adapter

molecule 1 (IBA-1) were purchased from Abcam (Cambridge, CB, UK). Mouse mAb against glial fibrillary acidic protein (GFAP) was purchased from Millipore Corp (Billerica, MA, USA), while goat anti-Rabbit IgG (H+L) Alexa Fluor 488 conjugate secondary antibody was from Cell Signaling Technology, Inc. (Beverly, MA, USA). Biotin-labeled goat anti-rabbit IgG, horseradish peroxidase (HRP)-labeled streptavidin, and diaminobenzidine (DAB) chromogenic kit were all purchased from Zhongshan Goldenbridge Biotechnology Co., Ltd. Goat anti-rabbit or anti-mouse IgG conjugated to IRDye™ (800CW) were from Licor biosciences (Lincoln, NE, USA). The BCA protein assay kit was from Pierce Chemical Company (Rockford, IL, USA), while TRIzol was purchased from Invitrogen, Inc. (Singapore). The first-strand complementary DNA (cDNA) synthesis kit was from Thermo Fisher Scientific (Waltham, MA, USA). In-situ Cell Death Detection Kit and Fluorescein was from Roche, Inc. (Roche, Germany). Enzyme-linked immunosorbent assay (ELISA) kits detecting TNF- α , IL-1 β , or IL-6, were from Jiancheng Bioengineering Institute (Nanjing, China).

Animals and Chronic Cerebral Hypoperfusion (CCH) Model

Adult Sprague–Dawley rats (male, 180–210 g), from the Beijing Vital River Laboratory Animal Technology Co., Ltd., were housed with accessible food and water ad libitum. Rats were maintained on a 12-h light/dark cycle, with the light on from 7:00 am to 7:00 pm. All animal experiments were performed according to the University's Policies on the Use of Animals and Humans in Neuroscience Research.

All rats were divided into the following four groups: the control group (Con; $n=12$), which only received saline (8 ml/kg weight; pH 7.0); bilateral common carotid arteries ligation group (2VO) ($n=14$), which received bilateral common carotid arteries ligation and equal volume of saline (pH 7.0); 2VO + Lut group ($n=14$), which received 2VO operation and luteolin treatment for 1 month since the 2VO operation; and Lut group ($n=12$), which only received the luteolin treatment for 1 month without the 2VO operation.

The rats were administered with chloral hydrate (0.4 g/kg) intraperitoneally for anesthetization. During surgery, temperature was maintained at 37 °C with a heating pad. After a ventral midline incision, both common carotid arteries were gently separated from the carotid sheath and vagus nerve [16]. Bilateral common carotid arteries were doubly ligated with 4-0 silk suture just below the carotid bifurcation, respectively. In control rats, a similar surgery was performed with no vessel ligation. After the surgery was finished, the rats were maintained at 37 °C until recovery. The surgery did not wholly or partially soften the brains of rats. A criterion of the 2VO model was that blood flow was reduced to 70%

below normal. To verify the 2VO model, we used a laser Doppler system to detect the level of blood flow.

Drug Treatment

Luteolin was dissolved in sodium hydrogen carbonate, adjusted pH value to 7.0, and a final concentration of luteolin solution was 3.75 mg/ml. On the second day after the construction of CCH model, rats were subjected to luteolin intraperitoneal injection (30 mg/kg weight) for 30 days from 2nd day after 2VO.

Morris Water Maze

After 30 days of cerebral hypoperfusion or luteolin treatment, the Morris water maze (MWM) was used to measure spatial memory. The rats were first trained in the MWM to find a hidden platform for 7 consecutive days, for 3 trials per day, with a 30-s interval from 2:00 to 8:00 pm. Each trial started with the rat in the middle of the outer round edge in one of the four quadrants facing the wall of the pool and ended when the animal climbed on the platform. The rats that could not find the platform in 60 s were guided to the platform. The rats' swimming pathways and latencies to find the hidden platform were recorded as previously reported using a video camera fixed to the ceiling of the room, 1.5 m above the water surface [17]. The scores of first trials to arrive the platform during the 7 days were recorded to evaluate the learning ability. For the memory retention test, the platform was removed and the place where the platform originally existed was recorded as the cued area in the software. Rats were placed in the 1st quadrant of the maze. The swimming pathway and latency to the first time to reach the cued area, the number of times crossing the cued area, and the total time in the 3rd quadrant was recorded.

Novel Object Recognition Test

Rats have the natural tendency to explore novel objects than familiar ones [18, 19]. Based on this discipline, the novel object recognition (NOR) test was developed to assess short-term memory deficits. The rats were placed in a 55 × 55 × 38 cm open-field box with black Plexiglas. Briefly, on day 1, two objects were symmetrically placed in box. The rats were habituated for 20 min to explore and familiarize the open-field arena. On day 2, two novel objects were placed at diagonal corners in the box and the rats were allowed to explore two similar objects for 5 min to acquire the objects information (containing the size, shape, and colors, etc.). After acquisition training, the rats were returned to cages for rest. On day 3, 24 h after the acquisition training, to test the memory retention on the two objects, one of the two familiar objects during acquisition training was replaced by a novel

object to form the novel and old objects. The rats were then placed in a box to explore familiar and novel objects for 5 min. The time spent exploring each object was recorded. A ratio of the time spent exploring the novel or old object over the total time spent exploring both objects was calculated. The exploration discrimination index was calculated as the time spent exploring the novel vs. old object over the total time spent exploring both objects [20, 21].

Electrophysiology

After the spatial memory retention test, rats were anaesthetized with urethane (1.6 g/kg, i.p.). Electrodes were implanted in the following coordinates: 3.4 mm posterior to the bregma and 3.5 mm lateral to the midline for the recording electrode, and 7.0 mm posterior to the bregma and 4.1 mm lateral to the midline for the stimulating electrode. The ground electrode was connected to the muscle contra lateral to the electrode sites. Recordings of field excitatory postsynaptic potential (fEPSPs) were made from the pyramidal neuron of CA3 region in response to stimulation of the perforant path (PP). The data acquisition system was triggered simultaneously to record all events. The sampling speed was 3 kHz for fEPSP recordings. The high-frequency stimulation protocol to induce LTP consisted of 10 trains of 15 stimuli (200 Hz), with 5-s intervals. This rather weak LTP induction protocol was chosen to prevent saturation of LTP, and thus, allow the possibility to detect improvements or impairments. Stimulation intensity was 60% of the max. fEPSP was analyzed by establishing an input–output correlation. LTP was measured as % of the baseline fEPSP slope, recorded over a 15-min period prior to application of high frequency stimulation (HFS). This value was taken as 100% of the EPSP slope, and all recorded values were normalized to this baseline value. PPF is considered to be triggered by pre-synaptic transmitter release facilitating processes [22], while later PPF is considered to be linked to γ -aminobutyric acid (GABA) interneuronal synaptic transmission [23, 24]. PPF was measured to analyze presynaptic functions and interneuron activity, as described by Gengler et al. [25]. Briefly, two stimuli were given at 60% of max fEPSP response. The interval between two stimuli was changed from 25 to 50, 80, 120, 160, and 200 ms to analyze PPF in relation to time. Data were normalized by the first fEPSP value and presented as ratio of the second fEPSP to the first fEPSP. Data were analyzed using Igor Pro 6.1 (WaveMetrics, Lake Oswego, Oregon) software.

Enzyme-Linked Immunosorbent Assay

The hippocampi were rapidly removed, homogenized, mixed with sample buffer, and then centrifuged at 12,000 \times g, for 10 min, at 25 °C. Inflammatory cytokines (TNF- α , IL-1 β ,

and IL-6) from the supernatant was detected using ELISA kit from Jiancheng Bioengineering Institute (Nanjing, China) according to manufacturers' protocols. The absorbance at 450 nm was determined by a Thermo Scientific microplate reader to calculate the concentration of inflammatory cytokines [26].

Measurement of MDA Content and Measurement of SOD and GPx Activity

MDA, which is generated by free radicals, is a lipid peroxidation marker. The MDA level was assayed to detect oxidative stress. Brain tissue were homogenized and the homogenate was reacted with thiobarbituric acid in assay kits at 95 °C. The supernatant was isolated by centrifuge, at 3500 rpm, for 10 min. According to manufacturers' protocols from Jiancheng Biotech Co., Ltd. (Nanjing, China) [27, 28], the level of MDA was calculated with the absorbance at 532 nm, which was measured using a Thermo Scientific microplate reader.

The brain homogenate was centrifuged at 12,000 rpm for 10 min at 4 °C. Supernatants were isolated and reacted with SOD assay kit at 37 °C for 20 min according to manufacturers' protocols. The absorbance at 450 nm of the supernatant was measured using a microplate reader to calculate the activity of SOD, according to manufacturers' protocols from Jiancheng Biotech Co., Ltd. (Nanjing, China).

The brain homogenate was centrifuged at 3500 rpm for 10 min at 4 °C. The supernatants were isolated and mixed with 20 μ mol/L glutathione and working solutions. The mixture incubated at room temperature for 15 min. The absorbance of the mixture at 412 nm was measured using a microplate reader to calculate the activity of GPx, according to manufacturers' protocols from Jiancheng Biotech Co., Ltd. (Nanjing, China).

Immunohistochemistry and Immunofluorescence

For immunohistochemical studies, rats were sacrificed with an overdose of chloral hydrate (1 g/kg) and perfused through aorta with 100 ml of 0.9% NaCl, followed by 400 ml phosphate buffer containing 4% paraformaldehyde. Brains were removed, post-fixed in perfusate overnight, and embedded in paraffin. Then, paraffin-embedded brain tissue was cut into 5- μ m sections on to slides. The slides were then rinsed in dimethylbenzene for dewaxing, and sequentially in 100, 100, 95, 90, 80, and 75% ethanol for rehydrating. Antigen retrieval was then performed by immersing the slides in 10 mmol/L citrate (pH 6), in a water bath at 95 °C, for 30 min. The sections of rat brains were then blocked with 0.3% H₂O₂ in absolute methanol for 10 min. Nonspecific sites were blocked with bovine serum albumin (BSA) for 30 min at room temperature. Sections were then incubated overnight at 4 °C with primary

antibodies, i.e., pAb IBA-1 (1:200). After washing with PBS, the sections were subsequently incubated with biotin-labeled secondary antibodies for 1 h at 37 °C. The immunoreaction was detected using horseradish peroxidase-labeled antibodies for 1 h at 37 °C and visualized with the diaminobenzidine tetrachloride system (brown color). The slices were then dehydrated in gradient ethanol, transparent in dimethylbenzene, and mounted by coating with neutral gum. A total of 4–5 consecutive sections from each brain were used. The images were observed using a microscope (Olympus BX60, Tokyo, Japan).

For immunofluorescence studies, rats were anaesthetized with an overdose of chloral hydrate (1 g/kg), perfused, fixed, and embedded in paraffin. Brains were cut into 5- μ m sections on to slides. The sections of rat brains were then blocked with 0.3% H₂O₂ in absolute methanol for 10 min. Nonspecific sites were blocked with BSA for 30 min at room temperature. Sections were then incubated overnight at 4 °C with primary antibodies, i.e., mAb GFAP (1:200). After washing with PBS, the sections were subsequently incubated with Alexa Fluor 488 conjugated secondary antibody secondary to develop the sections and observe neurons under a fluorescence microscope.

Klüver–Barrera Staining

Klüver–Barrera staining were performed on brain sections to measure white matter lesions of the corpus callosum, as previously described. Briefly, the sections were incubated with luxol fast blue. The severity of white matter lesions was graded for normalcy (Grade 0), disarrangement of nerve fibers (Grade 1), formation of marked vacuoles (Grade 2), and disappearance of myelinated fibers (Grade 3) [29].

Terminal Deoxynucleotidyl Transferase (TdT)-Mediated dUTP Nick End Labelling (TUNEL)

The 5- μ m rat brain section were also used to detect cell apoptosis. The slides were dewaxed, dehydrated using a gradient of alcohols, permeabilized in 10 mmol/L citrate (pH 6 at 95 °C) for 30 min. Then the In-situ Cell Death Detection Kit, Fluorescein (Roche, Germany) was applied to the slides, as described in the manufacturer's protocol. The slides were rinsed in PBS twice for 10 min each, incubated with the TUNEL reaction mixture for 60 min at 37 °C, and rinsed three times in PBS to stop the reaction. Apoptosis-positive cells were counted in three slices per rat using an Olympus microscope, at $\times 200$ magnification [30, 31].

Total RNA Extraction and Quantitative RT-PCR Analysis

Hippocampi tissue was separated from the rats' brain, frozen in liquid nitrogen, and stored at -80 °C until use. Total RNA

of 50 mg of hippocampi tissue was extracted using the TRIzol Reagent according to the manufacturer's protocol (Invitrogen, Singapore). First strand cDNA was synthesized from total RNA using a First-strand cDNA Synthesis Kit (Thermo Fisher Scientific, Waltham, Mass). The SYBR GREEN Mix reaction system was used for RT-PCR along with the forward primer, reverse primer, and cDNA. The reaction process included a pre-incubation step at 95 °C for 3 min; an amplification step of 43 cycles at 94 °C for 30 s, and then, at 56.8 °C and 72 °C for 30 s; and finally, an elongation step at 72 °C for 10 min. A melting curve was recorded to verify the absence of primer dimers. Glyceraldehyde 3-phosphate dehydrogenase (GAPDH) was used as the endogenous control. The levels of TNF- α , IL-1 β , and IL-6 RNA were assayed using the “ $\Delta\Delta C_t$ method” for relative expression.

Western Blot

For western blotting, rats were first decapitated. Then, the hippocampi were rapidly removed and homogenized. The extract was mixed with sample buffer, boiled for 10 min, and then centrifuged at 12,000 $\times g$ for 10 min at 25 °C. The protein concentration was estimated using a BCA Kit. The proteins were separated using 10% sodium dodecyl sulfate polyacrylamide gel electrophoresis (SDS-PAGE) and transferred to nitrocellulose membranes. The membranes were blocked with 5% non-fat milk and probed overnight with primary antibody at 4 °C, incubated with anti-rabbit or anti-mouse IgG conjugated to IRDye™ (800CW) (1:10,000) for 1 h at 4 °C, and visualized using the Odyssey Infrared Imaging System (Licor biosciences, Lincoln, NE, USA). The band intensities were quantified and normalized to β -actin. Values were expressed as intensity values ratio of control (i.e., as fold changes).

Statistics Analysis

Data were expressed as mean \pm standard error of mean (SEM) and analyzed using SPSS 12.0 statistical software (SPSS Inc., Chicago, Illinois, USA). The repeated-measures analysis of variance procedure was used to determine the statistical significance of differences in the mean learning latency between the three groups. A one-way analysis of variance followed by Dunnett's t-test was used to determine the statistical significance of differences of the means for other studies. Statistical significance was set at $P < 0.05$.

Results

Luteolin Could Prevent the CCH-Induced Increase in the Expression of Inflammatory Factors in the Hippocampus and Cortex

CCH upregulated the expression of pro-inflammatory factors in the brain, while luteolin, which is a natural flavonoid found in many plants, had anti-inflammatory activity. We detected TNF- α , IL-1 β , and IL-6 in the hippocampus or cortex homogenate using ELISA to investigate the anti-inflammatory effect of luteolin following CCH. Compared to the control group, the 2VO group had significantly increased levels of TNF- α , IL-1 β , and IL-6 in the hippocampus and cortex ($P < 0.01$) (Fig. 1a–f). Luteolin treatment, however, dramatically reduced TNF- α , IL-1 β , and

IL-6 in the hippocampus and cortex ($P < 0.05$ or $P < 0.01$) (Fig. 1a–f). We investigated the mRNA level of inflammatory factors through quantitative RT-PCR analysis. Compared to the control group, CCH distinctly enhanced the mRNA expression of inflammatory factors in the hippocampus and cortex ($P < 0.01$) (Fig. 2a–f). Luteolin treatment, however, dramatically reduced the mRNA levels of inflammatory factors in the hippocampus and cortex ($P < 0.05$ and $P < 0.01$, respectively) (Fig. 2a–f). These results indicated that luteolin had a strong anti-inflammatory effect on the brain after CCH.

Luteolin Could Prevent CCH-Induced Oxidative Stress in the Hippocampus and Cortex

To investigate whether luteolin could ameliorate CCH-induced oxidative stress in the brain, we measured the

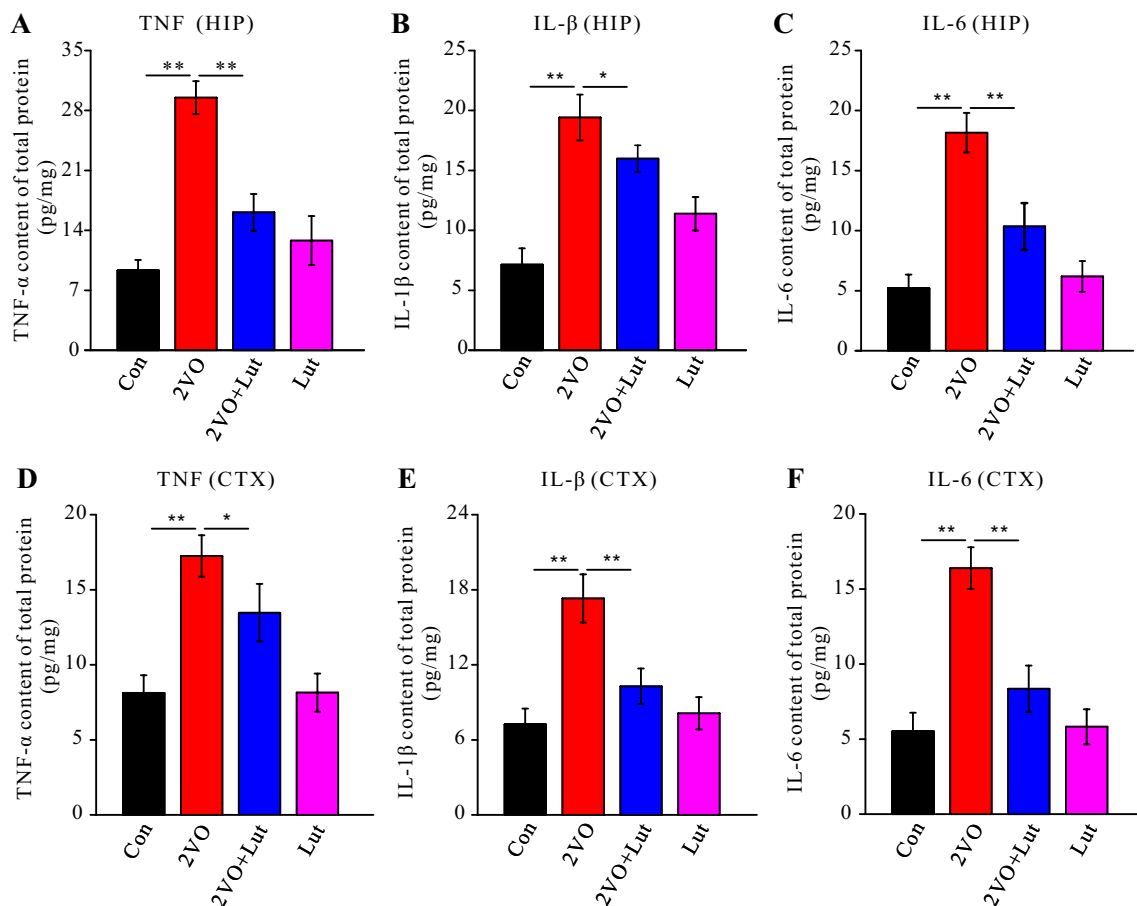


Fig. 1 Luteolin could decrease inflammation factors level of hippocampal and cortex after chronic cerebral hypoperfusion (CCH) in rats. After 1-month 2VO operation, the levels of TNF- α , IL-1 β , and IL-6 in hippocampal and cortex tissue, were detected using enzyme-linked immunosorbent assay (ELISA). **a–c** Levels of TNF- α , IL-1 β , and IL-6 in the hippocampal tissue of different groups (Con: n=4; 2VO: n=4; 2VO+Lut: n=5; Lut: n=4); **d–f** levels of TNF- α , IL-1 β ,

and IL-6 in the cortex tissue of different groups (Con: n=4; 2VO: n=4; 2VO+Lut: n=5; Lut: n=4). *HIP* hippocampus, *CTX* cortex. Con: sham group; 2VO: group receiving CCH using 2-vessel occlusion; 2VO+Lut: group receiving 2-vessel occlusion and luteolin treatment; Lut: sham group receiving luteolin treatment. Data are expressed as mean \pm SEM. * $P < 0.05$; ** $P < 0.01$ compared with the sham group or 2VO group

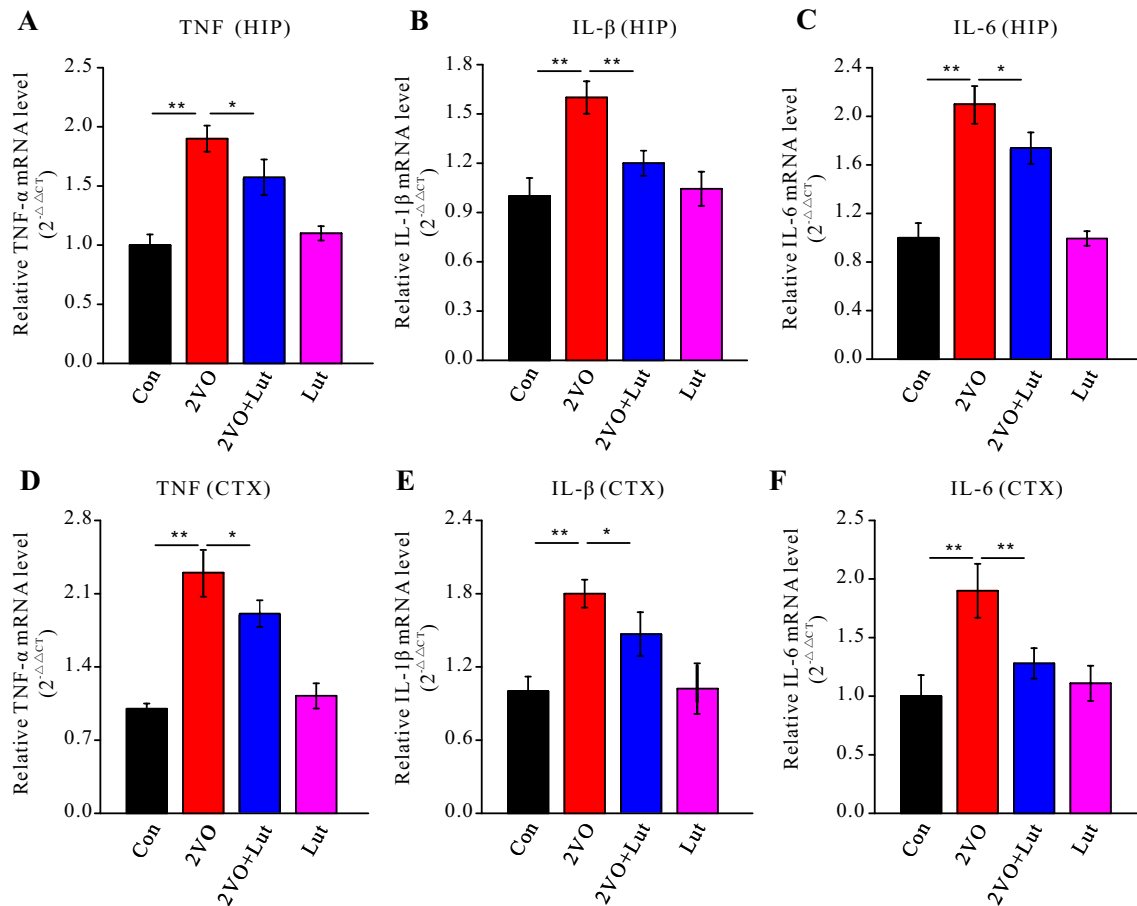


Fig. 2 Luteolin could prevent the mRNA increase of inflammation factors in the hippocampus and cortex in rats after chronic cerebral hypoperfusion (CCH). One month after the 2VO operation, the levels of TNF- α , IL-1 β , and IL-6 in hippocampus and cortex tissue, were detected using quantitative RT-PCR and analyzed using the $2^{-\Delta\Delta C_T}$ method. **a–c** mRNA levels of TNF- α , IL-1 β , and IL-6 in the hippocampal tissue of different groups (Con: n=4; 2VO: n=4; 2VO+Lut: n=5; Lut: n=4); **d–f** mRNA levels of TNF- α , IL-1 β ,

and IL-6 in cortex tissue (Con: n=4; 2VO: n=4; 2VO+Lut: n=5; Lut: n=4) of different groups. *HIP* hippocampus, *CTX* cortex. Con: sham group; 2VO: group receiving CCH using 2-vessel occlusion; 2VO+Lut: group receiving 2-vessel occlusion and luteolin treatment; Lut: sham group receiving luteolin treatment. Data are expressed as means \pm SEM. * $P < 0.05$; ** $P < 0.01$ compared with the sham group or 2VO group

level of MDA, i.e., an important oxidative stress marker, in the 2VO model and found that the MDA content in the hippocampus and cortex in 2VO was much higher than the control group (hippocampus: $(0.38 \pm 0.08$ vs. $0.81 \pm 0.06)$ nmol/mg protein, $P < 0.01$; cortex: $(0.42 \pm 0.02$ vs. $0.73 \pm 0.06)$ nmol/mg protein, $P < 0.01$). The MDA content of the hippocampus and cortex in the 2VO+Lut group, however, was much lower than in the 2VO group (hippocampus: $(0.59 \pm 0.07$ vs. $0.81 \pm 0.06)$ nmol/mg protein, $P < 0.01$; cortex: $(0.59 \pm 0.07$ vs. $0.73 \pm 0.06)$ nmol/mg protein, $P < 0.05$) (Fig. 3a–b). These findings suggested that luteolin could prevent the 2VO-induced oxidative stress in the brain. We also measured the activity of SOD and GPx, i.e., two important reductases, in the 2VO model, to further explore whether luteolin could regulate redox activity. Our data showed that SOD activity

in the hippocampus and cortex in the 2VO group was significantly lower than in the control group (hippocampus: $(0.18 \pm 0.021$ vs. $0.32 \pm 0.024)$ U/mg protein, $P < 0.01$; cortex: $(0.14 \pm 0.015$ vs. $0.25 \pm 0.018)$ U/mg protein, $P < 0.01$). SOD activity of hippocampus or cortex in 2VO+Lut group was much higher than it in 2VO group (hippocampus: $(0.28 \pm 0.019$ vs. $0.18 \pm 0.021)$ U/mg protein, $P < 0.01$; cortex: $(0.18 \pm 0.019$ vs. $0.14 \pm 0.015)$ U/mg protein, $P < 0.05$) (Fig. 3c, d). Thus, the CCH decreased SOD activity in the brain in the 2VO group, while luteolin treatment ameliorated this effect. Similarly, luteolin treatment also prevented the CCH-induced decrease of GPx activity in the brain (Fig. 3e–f). Taken together, our results suggested that luteolin could prevent the CCH-induced oxidative stress in the hippocampus and cortex.

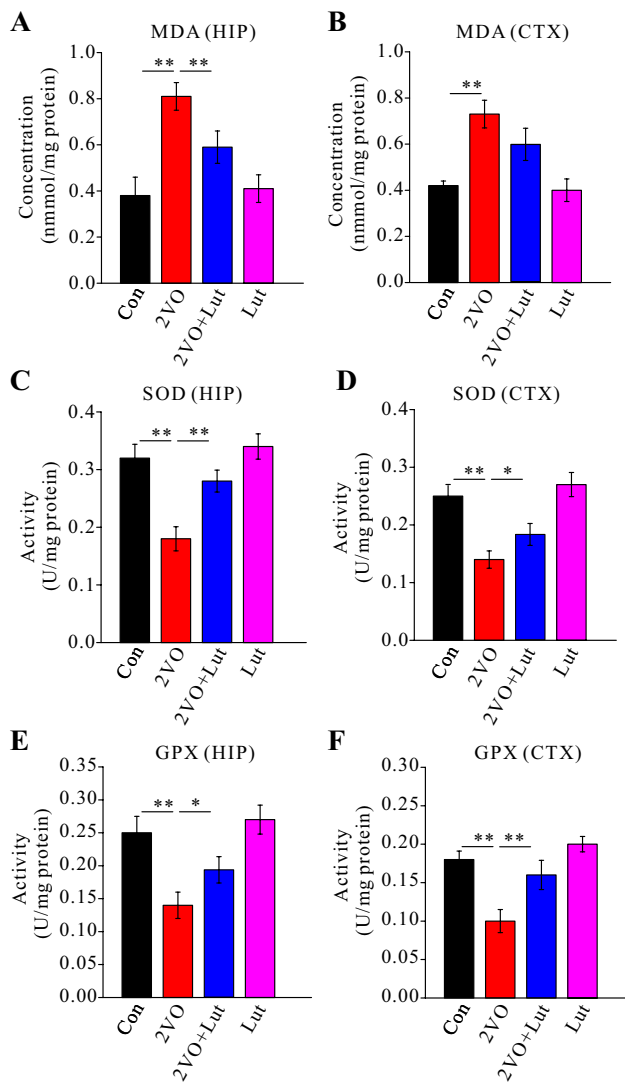


Fig. 3 Luteolin prevented the increase of the level of malondialdehyde (MDA) and improved the activity of superoxide dismutase (SOD) and glutathione peroxidase (GPx) in the hippocampus and cortex in rats after chronic cerebral hypoperfusion (CCH). One month after the 2VO operation, the levels of MDA and activity of SOD and GPx in hippocampal and cortex tissue, were measured using enzyme-linked immunosorbent assay (ELISA) and enzyme activity assay, respectively. **a, b** MDA levels in hippocampal and cortex tissue of different groups (Con: n=4; 2VO: n=4; 2VO+Lut: n=5; Lut: n=4); **c, d** activity assay of SOD in hippocampal and cortex tissue of different groups (Con: n=4; 2VO: n=4; 2VO+Lut: n=5; Lut: n=4). **e, f** activity assay of GPx in hippocampal and cortex tissue of different groups (Con: n=4; 2VO: n=4; 2VO+Lut: n=5; Lut: n=4). *HIP* hippocampus, *CTX* cortex. Con: sham group; 2VO: group receiving CCH using 2-vessel occlusion; 2VO+Lut: group receiving 2-vessel occlusion and luteolin treatment; Lut: sham group receiving luteolin treatment. Data are expressed as mean ± SEM. *P < 0.05; **P < 0.01 compared with the sham group or 2VO group

Luteolin Could Prevent CCH-Induced Microglia Over-activation and Astrogliosis in the Hippocampus and Cortex

Inflammatory factors could activate microglia, which in turn could generate more inflammatory factors, forming pernicious feedback. Based on the anti-inflammatory effect of luteolin, we explored whether luteolin could prevent the microglia over-activation in the hippocampus and cortex. An increased level of IBA-1 is an important marker of microglia over-activation. First, we measured the IBA-1 expression level using Western blot. The data demonstrated that the IBA-1 level in the 2VO group was significantly higher than that in the control group ($P < 0.01$) (Fig. 4a–b). Luteolin treatment noticeably reduced the IBA-1 level than in the 2VO group ($P < 0.01$) (Fig. 4a–b). IBA-1 immunohistochemistry staining was used to determine the distribution of over-activated microglia. The result demonstrated that the IBA-1 positive cells in the 2VO group were much higher than that in the control group ($P < 0.01$) (Fig. 4c, d). The number of IBA-1 positive cells in the 2VO + Lut group were much higher than in the 2VO group ($P < 0.01$) (Fig. 4c, d).

Generally, inflammation activates the proliferation and activation of astrocytes, i.e., astrogliosis, which could secrete pro-inflammatory factors. We measured GFAP expression level using western blot to further investigate whether luteolin could inhibit CCH-induced astrogliosis in the brain. The data showed that GFAP level in the 2VO group was significantly higher than that in the control group ($P < 0.01$) (Fig. 5a, b). The luteolin treatment noticeably reduced the GFAP level in the 2VO group ($P < 0.01$) (Fig. 5a, b). We observed GFAP-positive cells through immunofluorescence and found that the 2VO group had more GFAP-positive cells than the control group ($P < 0.01$) (Fig. 5c, d). The number of GFAP-positive cells in the 2VO + Lut group were much lower than in the 2VO group ($P < 0.01$) (Fig. 5a, b). Taken together, our results suggested that luteolin could prevent microglia over-activation and astrogliosis in the hippocampus and cortex after CCH.

CCH Did Not Induce Dramatic Apoptosis Hippocampus and Cortex

Serious inflammation can contribute to apoptosis in many tissues, especially the brain, given the vulnerability of neurons to various pessimal stimulations. To investigate whether CCH can contribute to neuronal apoptosis in the hippocampus and cortex, we observed apoptotic neurons using Tunnel staining and found there was no remarkable apoptosis in the hippocampus and cortex (Fig. 6a).

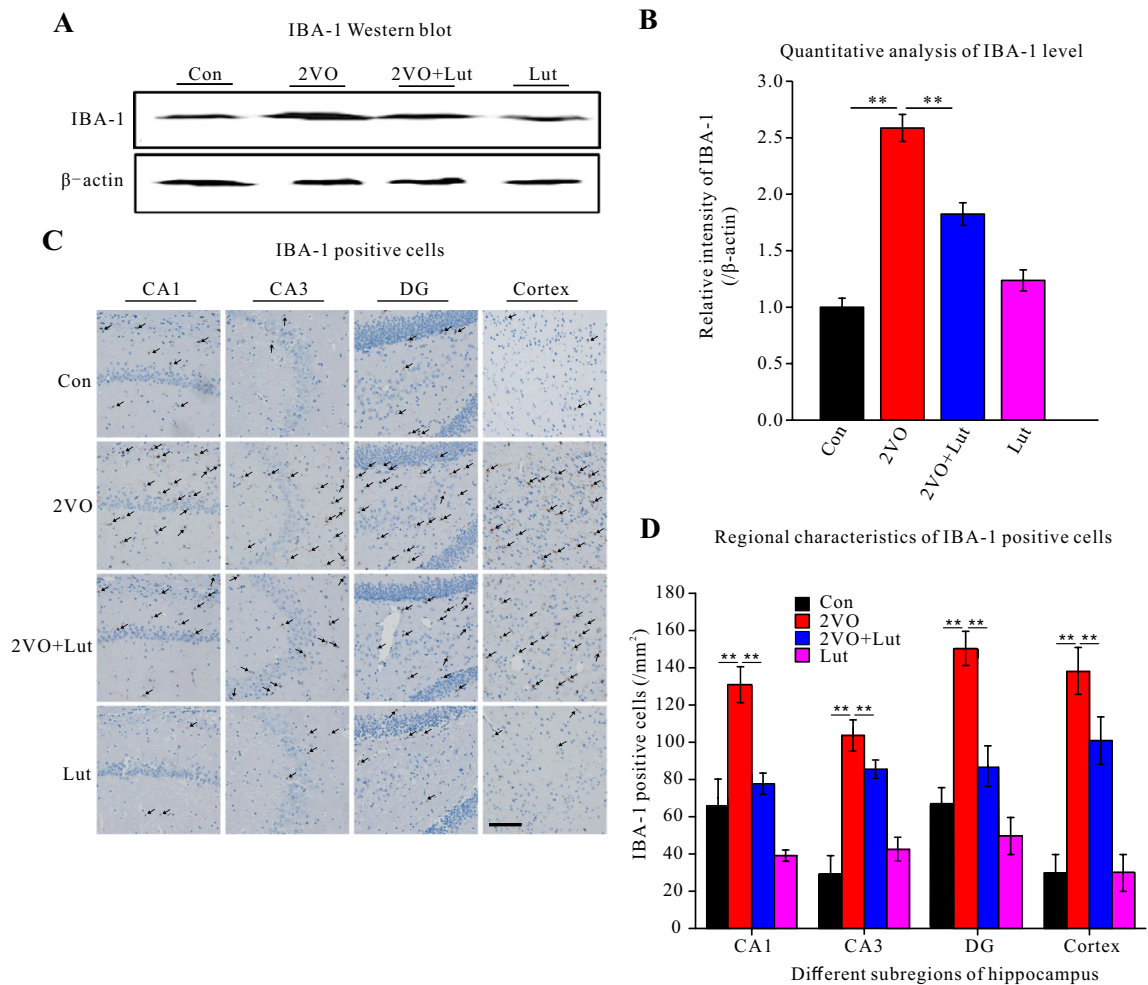


Fig. 4 Luteolin inhibited microglia activation in the rat hippocampus and cortex after chronic cerebral hypoperfusion (CCH). The rats were sacrificed 1 month after the 2VO operation, and brain tissue was collected, partly homogenized, and fixed to section. The homogenate of hippocampal and cortex tissue were assayed using western blotting with ionized calcium-binding adapter molecule 1 (IBA-1) antibody. IBA-1 positive glia were observed using immunohistochemistry staining. **a** IBA-1 level was detected by Western blot, and relatively

quantitatively analyzed (Con: $n=5$; 2VO: $n=4$; 2VO+Lut: $n=6$; Lut: $n=5$) (**b**). **c** IBA-1-positive glia were observed using immunofluorescence (bar = 100 μ m) and analyzed ($n=3$) (**d**). Con: the sham group; 2VO: group receiving CCH using 2-vessel occlusion; 2VO+Lut: group receiving 2-vessel occlusion and luteolin treatment; Lut: sham group receiving luteolin treatment. Data are expressed as mean \pm SEM. * $P < 0.05$; ** $P < 0.01$ compared with the sham group or 2VO group

Luteolin Could Prevent CCH-Induced White Matter Lesions

We used Klüver–Barrera staining to investigate corpus callosum nerve fibers and determine the white matter lesion grade. Our data showed that the lesion grade in the 2VO group was dramatically higher than of the control group (0.6 ± 0.07 vs. 2.8 ± 0.36 , $P < 0.01$); the lesion grade of the 2VO+Lut group, however, was significantly lower than that of the 2VO group (1.7 ± 0.25 vs. 2.8 ± 0.36 , $P < 0.01$) (Fig. 6b, c). Thus, this finding indicated that luteolin treatment could prevent CCH-induced white matter lesions.

Luteolin Could Prevent the CCH-Induced Learning and Memory Deficits

Chronic inflammation in the brain impairs cognition. Thus, we measured learning and short-term memory using MWM and NOR, respectively, to investigate whether the anti-inflammatory effect of luteolin could inhibit cognitive dysfunction after CCH. The MWM results demonstrated that the 2VO group took significantly longer than the control to reach the platform during the 3rd to 7th trail day ($P < 0.01$) (Fig. 7a). The 2VO+Lut group, however, spent significantly shorter than the 2VO group during the 3th to

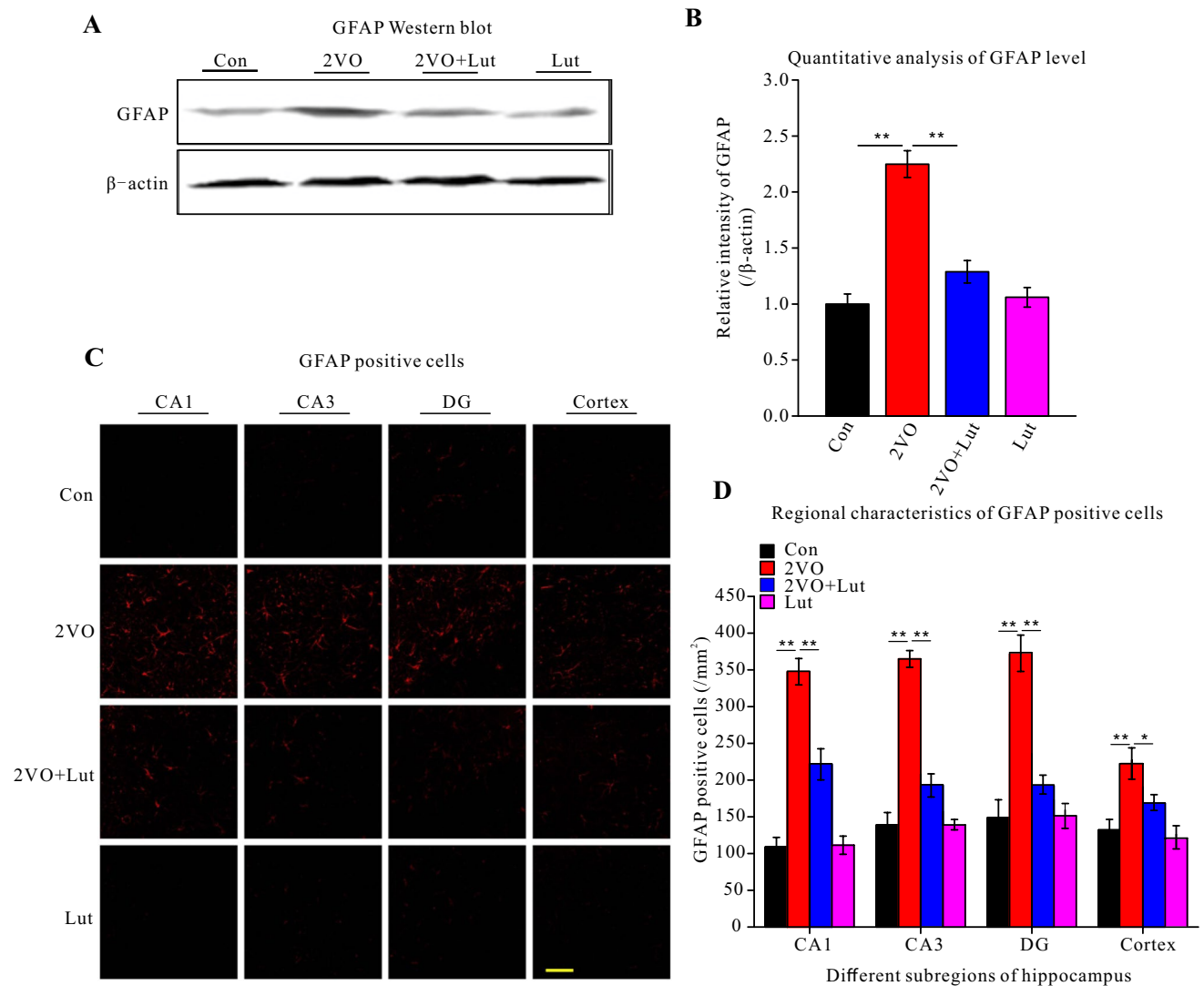


Fig. 5 Luteolin inhibited astrogliosis in the hippocampus and cortex in rats after chronic cerebral hypoperfusion (CCH). The hippocampal and cortex tissue homogenates were assayed using western blotting with glial fibrillary acidic protein (GFAP) antibody. GFAP-positive glia were observed using immunohistochemistry staining. **a** GFAP level detected using western blot and relatively quantitatively analyzed (Con: n=5; 2VO: n=4; 2VO+Lut: n=6; Lut: n=5) (**b**); **c** the

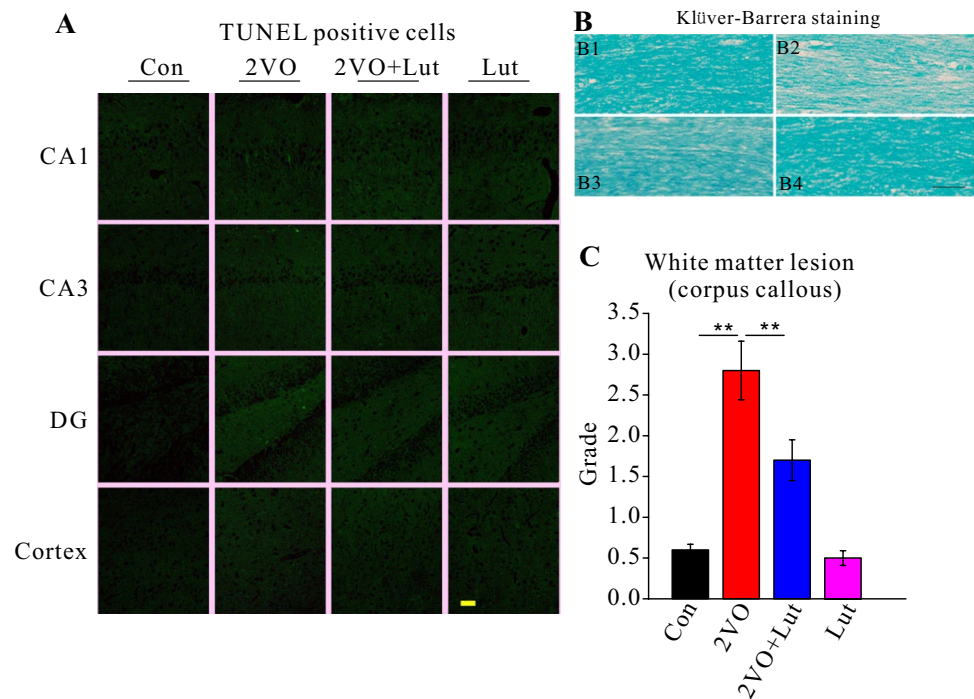
section was developed using a GFAP antibody and GFAP-positive glia and astrocytes were observed using immunofluorescence (bar =50 μm) and analyzed (n=3) (**d**). Con: sham group; 2VO: group receiving CCH using 2-vessel occlusion; 2VO+Lut: group receiving 2-vessel occlusion and luteolin treatment; Lut: sham group receiving luteolin treatment. Data are expressed as mean ± SEM. *P < 0.05; **P < 0.01 compared with the sham group or 2VO group

7th trail day (3rd to 4th day and 7th day, *P* < 0.05; 6th day, *P* < 0.01) (Fig. 7a). After 7-day training, when the platform was standing in the third quadrant or removed, the short-term memory test showed that rats in the 2VO group took distinctly longer than rats in the control group to reach the platform (*P* < 0.01). Rats in the 2VO+Lut group, however, spent significantly shorter than rats that underwent CCH to reach the platform (*P* < 0.05) (Fig. 7b, e). Both the duration the rats stayed in the third quadrant (Fig. 7c) and crossed the platform area (Fig. 7d) were significantly lower for the 2VO group than the control group (*P* < 0.01). The staying time and times crossing the platform of the 2VO+Lut

group, however, was longer than the 2VO group (*P* < 0.05 and *P* < 0.01, respectively) (Fig. 7c, d). These suggested that luteolin could prevent CCH-induced spatial learning deficits and memory dysfunction.

We used the NOR test to measure the anti-inflammatory effect of luteolin on CCH-induced learning and memory deficits. The ratio of time spent sniffing and touching new objects to total time of the 2VO group was significantly longer than for the control (*P* < 0.01) (Fig. 7f), whereas the ratio for the 2VO+Lut group was significantly shorter than for the 2VO group (*P* < 0.01) (Fig. 7f). In contrast, the time spent sniffing and touching old object to total time

Fig. 6 No obvious apoptosis was present in the rat hippocampus and cortex after chronic cerebral hypoperfusion (CCH). Brain paraffin sections (5 μ m) were stained using the Tunnel staining kit. Tunnel-positive cells were observed using immunofluorescence (bar = 100 μ m) and analyzed (n = 3) (a). Brain paraffin sections (5 μ m) were stained using luxol fast blue staining (b) grading of the degree of white matter (c). Con: sham group; 2VO: group receiving CCH using 2-vessel occlusion; 2VO + Lut: group receiving 2-vessel occlusion and luteolin treatment; Lut: sham group receiving luteolin treatment. B1: Con; B2: 2VO; B3: 2VO + Lut; B4: Lut. Data are expressed as means \pm SEM. * $P < 0.05$; ** $P < 0.01$ compared with the sham group or 2VO group



was significantly shorter for the 2VO group than that for the control ($P < 0.01$) (Fig. 7g), whereas the ratio in the 2VO + Lut group was significantly longer than in the 2VO group ($P < 0.05$) (Fig. 7g). Finally, the exploration discrimination index of the 2VO group was evidently lower than that of the control group, while the exploration discrimination index of the 2VO + Lut was higher than that of the 2VO group ($P < 0.01$) (Fig. 7h). These data suggested that the anti-inflammatory effect of luteolin could improve the CCH-induced deficit of learning and memory.

Luteolin Could Prevent CCH-Induced LTP Dysfunction

LTP, which reflects synaptic plasticity, is a critical electrophysiological mechanism of learning and memory [32, 33]. We studied LTP changes to investigate the electrophysiological mechanisms of the anti-inflammatory effect of luteolin on CCH-induced learning and memory deficits. The fEPSP was recorded, measured, and analyzed. After HFS, the fEPSPs of the control, 2VO, 2VO + Lut, and Lut groups were 192.86 ± 11.58 , 152.51 ± 12.47 , 179.67 ± 14.36 , and $187.92 \pm 9.29\%$ of the pre-HFS value, respectively (Fig. 8a). The fEPSPs were noticeably low in the 2VO group than that in the control group ($P < 0.01$). Further, fEPSPs were significantly higher in the 2VO + Lut than that in the 2VO group ($P < 0.05$) (Fig. 8b). These results suggested that the anti-inflammatory effect of luteolin might prevent CCH-induced LTP dysfunction.

Luteolin Could Prevent the Dysfunction of Presynaptic Transmitter Release Due to CCH

PPF was enhanced by dysfunctional pre-synaptic transmitter release [22]. We recorded and analyzed the PPF level in vivo in the hippocampus to investigate whether anti-inflammatory effect of luteolin improved the CCH-induced dysfunction of presynaptic transmitter release. At the 25, 50, 80, 120, 160, and 200 ms intervals, the ratios of EPSP2 and EPSP1 were all observably larger for the 2VO group than for the control group (25 and 120 ms, $P < 0.05$; 50, 80, 160, and 200 ms, $P < 0.01$) (Fig. 8c). The ratios of EPSP2 and EPSP1 in the 2VO + Lut were remarkably lower than those of the 2VO group (50 ms, $P < 0.01$; 25, 80, 160, and 200 ms, $P < 0.05$) (Fig. 8c). These results suggested that the anti-inflammatory effect of luteolin improved the CCH-induced dysfunction of presynaptic transmitter release.

Discussion

Our current study demonstrated that luteolin could decrease the level of inflammatory factors, such as TNF-1 α , IL-1 β , and IL-6, in the brain. Further, it enhanced SOD and GPX activities and reduced MDA. Luteolin also reduced microglia over-activation and astrogliosis in the hippocampus and cortex following CCH. However, there was no remarkable apoptosis in the brain following CCH. Luteolin also ameliorated CCH-induced white matter, PPF, and LTP changes, and spatial learning and memory deficits.

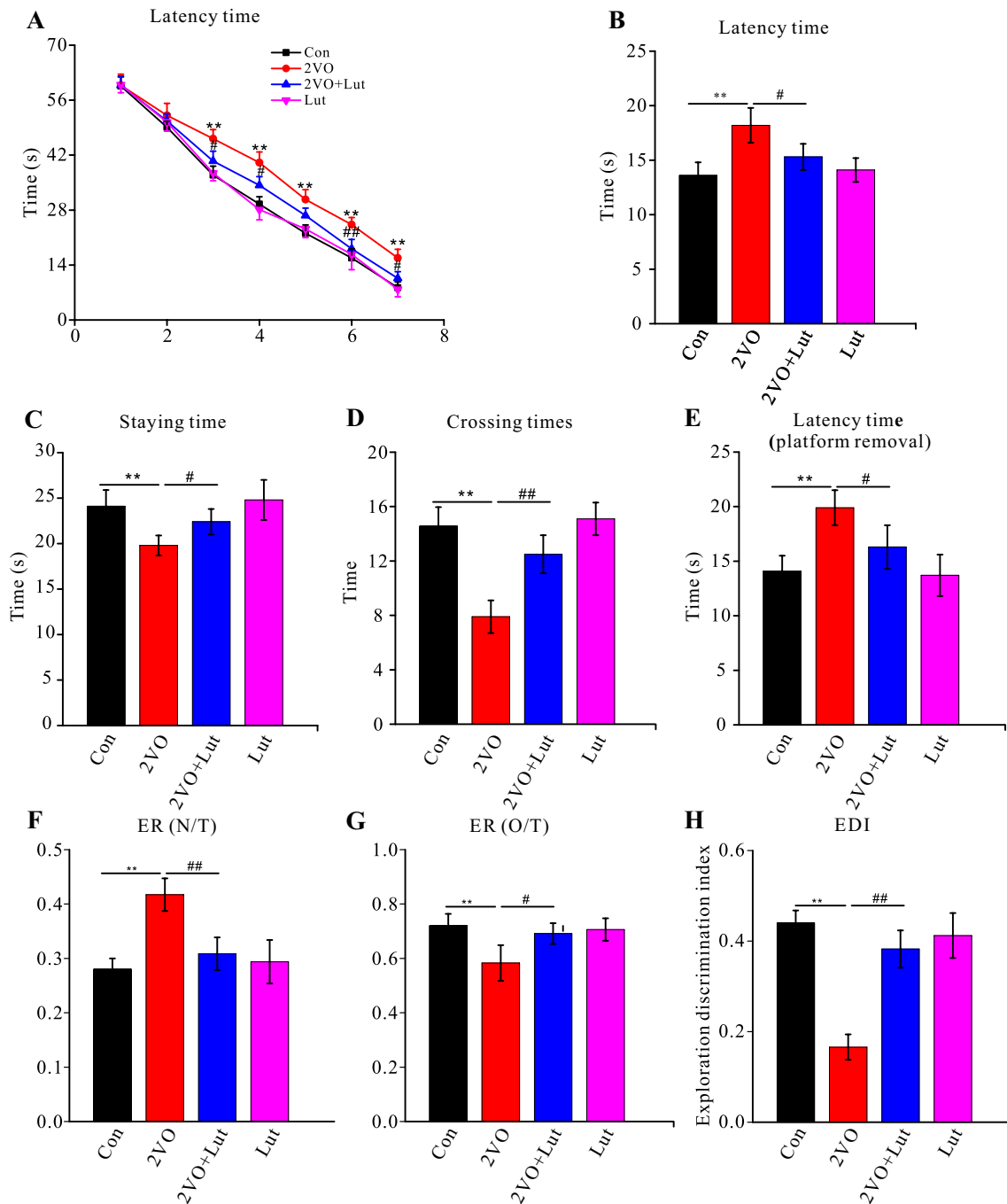
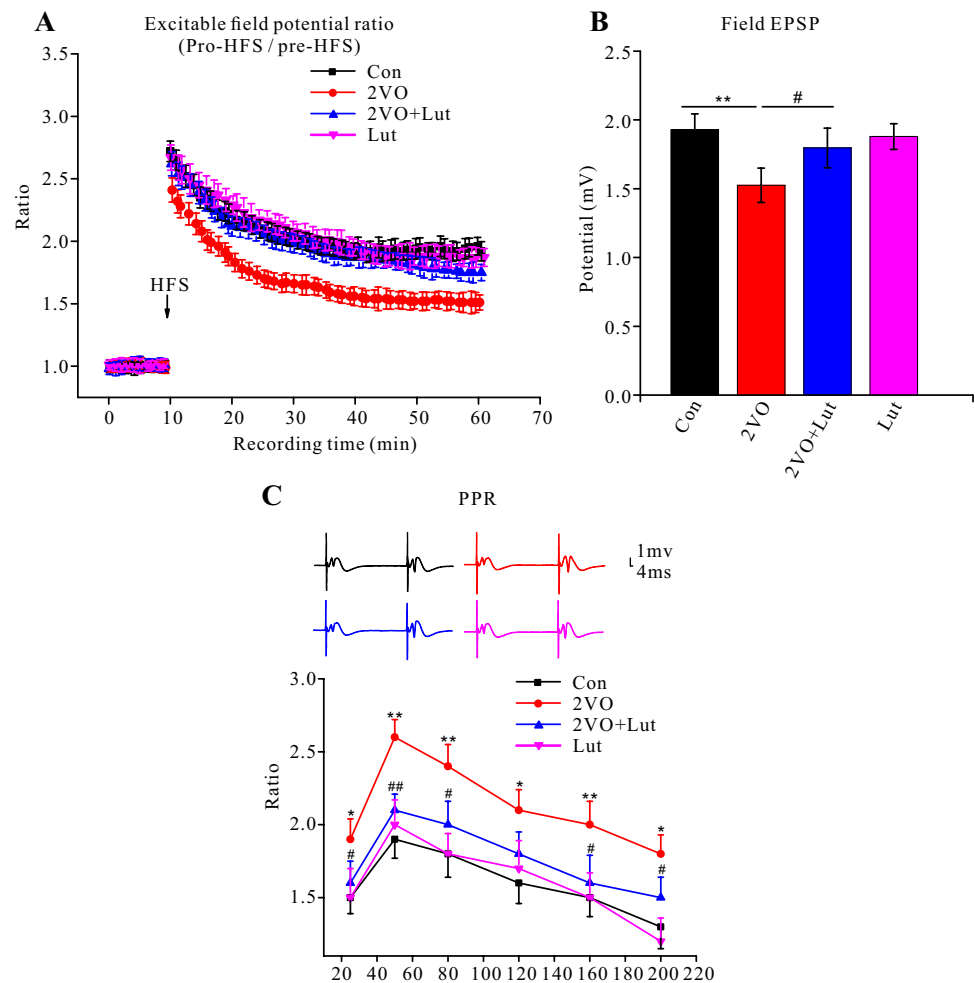


Fig. 7 Luteolin improved chronic cerebral hypoperfusion (CCH)-induced spatial learning and memory retention impairments in rats. At 1 month after CCH, learning and short memory were tested using the Morris water maze (MWM) and probe test. During the MWM test, the escape latency time and crossing times of the targeted area during learning training trails from 1st to 7th were recorded (a). To test short memory, the latency to reach the platform area (platform in pool) (b), staying time in the objective area (c), duration spent crossing the platform area (d), and latency to reach the platform area (removed platform) (e) were recorded and analyzed. During

probe test, the time spent with new and old objects was recorded. The time exploration ratio (ER) [new object time (N)/total time (T)] (f), exploration ratio (old object time/total time) [ER (O/T)] (g), and exploration discrimination index (EDI) (h) were calculated. Con: sham group; 2VO: group receiving CCH using 2-vessel occlusion; 2VO+Lut: group receiving 2-vessel occlusion and luteolin treatment; Lut: sham group receiving luteolin treatment. Data are expressed as mean±SEM (Con: n=12; 2VO: n=11; 2VO+Lut: n=12; Lut: n=12). **P<0.01 compared with the Con group; #P<0.05 or ##P<0.01 compared with the 2VO group

Fig. 8 Luteolin improved chronic cerebral hypoperfusion (CCH)-induced long-term potential impairments in rats. After the memory retention test, the field excitatory postsynaptic potential (EPSP) slope was recorded in the hippocampus (a). Relative field EPSP slopes were analyzed (b). Paired pulse was recorded and analyzed (c). Con: sham group; 2VO: group receiving CCH using 2-vessel occlusion; 2VO+Lut: group receiving 2-vessel occlusion and luteolin treatment; Lut: sham group receiving luteolin treatment. Data are expressed as mean \pm SEM (Con: n = 11; 2VO: n = 10; 2VO+Lut: n = 10; Lut: n = 11). * $P < 0.05$ or and ** $P < 0.01$ compared with the Con group; # $P < 0.05$ or ## $P < 0.01$ compared with the 2VO group



CCH increased the level of TNF-1 α , IL-1 β , IL-6, and MDA in the brain. Oxidative stress and inflammation play an important pathogenic role in brain dysfunction following CCH [34–36]. Free radicals produced by the enzyme nicotinamide adenine dinucleotide phosphate oxidase due to the lack of energy are responsible for CCH-induced cerebrovascular alterations [28]. Free radicals induce inflammation through the activation of redox-sensitive pro-inflammatory transcription factors and production of cytokines. Inflammation can also boost oxidative stress by upregulating the expression of reactive oxygen species and downregulating antioxidant defenses [34]. With CCH, the brain is in a long-term inflammation stimulation state, which affects brain function. The increase in PPF indicated that the basic neuronal transmission was impaired because of the less pre-synaptic vesicle release. In our study, CCH increased PPF and impaired learning and memory impairment. Luteolin however, decreased PPF and inflammation, which suggested that inflammation after CCH induced neuronal dysfunction.

The central structure of luteolin, which is an important flavone, consists of two phenyl rings joined by a pyran ring, and is present in broccoli, pepper, thyme, and celery [35].

Flavones can re-establish the inhibition of redox regulation proteins, transcription factors, and signaling cascades by oxidative stress [36]. A previous study demonstrated that luteolin had anti-inflammatory activity due to inhibition of tyrosine phosphorylation and protein kinase B phosphorylation, activation of NF- κ B and nuclear translocation of NF- κ B p65 subunit [35], activation of mitogen-activated protein kinase (MAPK), and degradation of inhibitor of kappa B- α (I κ B- α) after LPS treatment [34]. Moreover, luteolin significantly inhibited the LPS-induced DNA binding activity of activating protein-1 (AP-1) [37]. Through these mechanisms, luteolin finally inhibited the generation of inflammation cytokines, such as TNF-1 α , IL-1 β , IL-6, and COX2 [34, 37]. In our study, we also demonstrated that luteolin inhibited inflammation cytokines and oxidative stress. Although we did not investigate the underlying mechanisms, we postulated that luteolin may play an anti-inflammatory role in the brain after CCH through similar mechanisms.

Glia in the central nervous system maintains brain homeostasis, regulates neuronal function, and counter-strike pathogenic or environmental invasions [38]. As innate immune cells in the brain, microglia respond to oxidative stress and

inflammation and propagate cascade inflammatory signals, which consequently produces cytokines and inflammatory mediators [38]. The increase in astrocyte reactivity in response to pathogen and cerebral ischemia, is termed astrogliosis [39], which led to morphology changes, enhanced expression of GFAP, and secretion of inflammatory mediators [40–44]. As a result, the negative feedback of the exaggerated inflammatory response, due to astrogliosis, deteriorates synaptic plasticity, cognition and behavior. Thus, in the CCH brain, the activation of microglia and astrocytes due oxidative stress and inflammation consequently leads to cognition deficit. However, in the current study, luteolin abated oxidative stress, inflammation, and the activation of microglia and astrocytes. This consequently suspended the negative feedback of exaggerated inflammatory response to improve cognition. However, there was no apoptosis in the rat brain following CCH, which is a mild long-lasting ischemic process. This indicated that CCH did not initiate apoptosis or induce protective/impaired mechanisms. However, since we detected apoptosis in only 1 month, this does not mean that a longer time hypoperfusion (> 1 month) could not induce apoptosis. This remains to be validated in future studies.

Given the location depth, white matter was vulnerable to hypoperfusion and formed lesion [45]. The activation of microglia following CCH could also impair white matter due to the generation of inflammatory factors and phages [46]. Microstructural white matter integrity was positively associated with cognitive performance and white matter microstructure lesion could predict cognitive decline. Thus, maintaining better white matter integrity could preserve better cognition [47]. Oxidative stress and inflammation, glia activation in the white matter, and demyelination, axonal loss, or axonal breakdown, especially in the fornix body, impeded electric and chemistry signal transmission connecting the hippocampus and other brain areas. Further this impaired the neural circuit and decreased neural plasticity. These changes finally impaired cognition. In the current study, we found that luteolin could protect white matter and decrease CCH-induced inflammation, which suggested luteolin maybe inhibit white matter lesion by reducing CCH-induced inflammation. Stable LTP is established on the basis of normal function of neuronal function and nerve fibers. Luteolin could protect PPF and LTP, and reduced neuroinflammation and oxidative stress after CCH, which suggested that it could protect the transmission of neural signals to improve synaptic plasticity by inhibiting CCH-induced neuroinflammation. Apart from its anti-inflammatory effects, a neurotrophic or other effects of luteolin remains to be investigated in the future.

In summary, we demonstrated that luteolin decreased inflammatory factors, like TNF-1 α , IL-1 β , and IL-6, enhanced SOD and GPx activities, and reduced MDA.

Further, luteolin reduced CCH-induced microglia over-activation and astrogliosis in the hippocampus and cortex, and protected against CCH-induced changes in white matter, PPF, LTP, spatial learning, and memory. Our study suggested luteolin maybe a preferable anti-inflammatory agent to protect against CCH-induced changes in cognitive function and synaptic plasticity.

Acknowledgements This work was supported in part by Grants from the National Natural Science Foundation of China (NSFC) (81400891).

Compliance with Ethical Standards

Conflict of interest All authors declare that there are no conflicts of interest.

References

1. Tang H, Gao Y, Zhang Q, Nie K, Zhu R, Gao L et al (2017) Chronic cerebral hypoperfusion independently exacerbates cognitive impairment within the pathogenesis of Parkinson's disease via microvascular pathologies. *Behav Brain Res* 333:286–294
2. Choi BR, Lee SR, Han JS, Woo SK, Kim KM, Choi DH et al (2011) Synergistic memory impairment through the interaction of chronic cerebral hypoperfusion and amyloid toxicity in a rat model. *Stroke* 42(9):2595–2604
3. Fernandez-Ruiz A, Oliva A, Nagy GA, Maurer AP, Berenyi A, Buzsaki G (2017) Entorhinal-CA3 dual-input control of spike timing in the hippocampus by theta-gamma coupling. *Neuron* 93(5):1213–1226.e5
4. Hase Y, Craggs L, Hase M, Stevenson W, Slade J, Lopez D et al (2017) Effects of environmental enrichment on white matter glial responses in a mouse model of chronic cerebral hypoperfusion. *J Neuroinflammation* 14(1):81
5. Wang J, Zhang HY, Tang XC (2010) Huperzine A improves chronic inflammation and cognitive decline in rats with cerebral hypoperfusion. *J Neurosci Res* 88(4):807–815
6. Shimoi K, Okada H, Furugori M, Goda T, Takase S, Suzuki M et al (1998) Intestinal absorption of luteolin and luteolin 7-O-beta-glucoside in rats and humans. *FEBS Lett* 438(3):220–224
7. Kwon Y (2017) Luteolin as a potential preventive and therapeutic candidate for Alzheimer's disease. *Exp Gerontol* 95:39–43
8. Kotanidou A, Xagorari A, Bagli E, Kitsanta P, Fotsis T, Papapetropoulos A et al (2002) Luteolin reduces lipopolysaccharide-induced lethal toxicity and expression of proinflammatory molecules in mice. *Am J Respir Crit Care Med* 165(6):818–823
9. Xagorari A, Papapetropoulos A, Mauromatis A, Economou M, Fotsis T, Roussos C (2001) Luteolin inhibits an endotoxin-stimulated phosphorylation cascade and proinflammatory cytokine production in macrophages. *J Pharmacol Exp Ther* 296(1):181–187
10. Nunes C, Almeida L, Barbosa RM, Laranjinha J (2017) Luteolin suppresses the JAK/STAT pathway in a cellular model of intestinal inflammation. *Food Funct* 8(1):387–396
11. Xiong J, Wang K, Yuan C, Xing R, Ni J, Hu G et al (2017) Luteolin protects mice from severe acute pancreatitis by exerting HO-1-mediated anti-inflammatory and antioxidant effects. *Int J Mol Med* 39(1):113–125
12. Hytti M, Piippo N, Korhonen E, Honkakoski P, Kaarniranta K, Kauppinen A (2015) Fisetin and luteolin protect human retinal pigment epithelial cells from oxidative stress-induced cell death and regulate inflammation. *Sci Rep* 5:17645

13. Zhang JX, Xing JG, Wang LL, Jiang HL, Guo SL, Liu R (2017) Luteolin inhibits fibrillary beta-amyloid1-40-induced inflammation in a human blood-brain barrier model by suppressing the p38 MAPK-mediated NF-kappaB signaling pathways. *Molecules* 22(3):334. <https://doi.org/10.3390/molecules22030334>
14. Lin TY, Lu CW, Wang SJ (2016) Luteolin protects the hippocampus against neuron impairments induced by kainic acid in rats. *Neurotoxicology* 55:48–57
15. Paterniti I, Impellizzeri D, Di Paola R, Navarra M, Cuzzocrea S, Esposito E (2013) A new co-ultramicrosized composite including palmitoylethanolamide and luteolin to prevent neuroinflammation in spinal cord injury. *J Neuroinflammation* 10:91
16. Briones TL, Therrien B, Metzger B (2000) Effects of environment on enhancing functional plasticity following cerebral ischemia. *Biol Res Nurs* 1(4):299–309
17. Morris R (1984) Developments of a water-maze procedure for studying spatial learning in the rat. *J Neurosci Methods* 11(1):47–60
18. Asuni AA, Boutajangout A, Quartermain D, Sigurdsson EM (2007) Immunotherapy targeting pathological tau conformers in a tangle mouse model reduces brain pathology with associated functional improvements. *J Neurosci* 27(34):9115–9129
19. Scholtzova H, Wadghiri YZ, Douadi M, Sigurdsson EM, Li YS, Quartermain D et al (2008) Memantine leads to behavioral improvement and amyloid reduction in Alzheimer's-disease-model transgenic mice shown as by micromagnetic resonance imaging. *J Neurosci Res* 86(12):2784–2791
20. Scholtzova H, Do E (2017) Innate immunity stimulation via toll-like receptor 9 ameliorates vascular amyloid pathology in Tg-SwDI mice with associated cognitive benefits. *J Neurosci* 37(4):936–959
21. Gonzalez-Vera JA, Medina RA, Martin-Fontecha M, Gonzalez A, de la Fuente T, Vazquez-Villa H et al (2017) A new serotonin 5-HT6 receptor antagonist with procognitive activity—importance of a halogen bond interaction to stabilize the binding. *Sci Rep* 7:41293
22. Chen Y, Chad JE, Wheal HV (1996) Synaptic release rather than failure in the conditioning pulse results in paired-pulse facilitation during minimal synaptic stimulation in the rat hippocampal CA1 neurones. *Neurosci Lett* 218(3):204–208
23. Schulz PE, Cook EP, Johnston D (1995) Using paired-pulse facilitation to probe the mechanisms for long-term potentiation (LTP). *J Physiol Paris* 89(1):3–9
24. Tsai ML, Shen B, Leung LS (2008) Seizures induced by GABAB-receptor blockade in early-life induced long-term GABA(B) receptor hypofunction and kindling facilitation. *Epilepsy Res* 79(2–3):187–200
25. Gengler S, Hamilton A, Holscher C (2010) Synaptic plasticity in the hippocampus of a APP/PS1 mouse model of Alzheimer's disease is impaired in old but not young mice. *PLoS ONE* 5(3):e9764
26. Dong YF, Chen ZZ, Zhao Z, Yang DD, Yan H, Ji J et al (2016) Potential role of microRNA-7 in the anti-neuroinflammation effects of nicorandil in astrocytes induced by oxygen-glucose deprivation. *J Neuroinflammation* 13(1):60
27. Zhang GL, Deng JP, Wang BH, Zhao ZW, Li J, Gao L et al (2011) Gypenosides improve cognitive impairment induced by chronic cerebral hypoperfusion in rats by suppressing oxidative stress and astrocytic activation. *Behav Pharmacol* 22(7):633–644
28. Korani MS, Farbood Y, Sarkaki A, Moghaddam HF, Mansouri MT (2014) Protective effects of gallic acid against chronic cerebral hypoperfusion-induced cognitive deficit and brain oxidative damage in rats. *Eur J Pharmacol* 733:62–67
29. Toyama K, Koibuchi N, Hasegawa Y, Uekawa K, Yasuda O, Sueta D et al (2015) ASK1 is involved in cognitive impairment caused by long-term high-fat diet feeding in mice. *Sci Rep* 5:10844
30. Wang Z, Qiu Z, Gao C, Sun Y, Dong W, Zhang Y et al (2017) 2,5-Hexanedione downregulates nerve growth factor and induces neuron apoptosis in the spinal cord of rats via inhibition of the PI3K/Akt signaling pathway. *PLoS ONE* 12(6):e0179388
31. Duris K, Manaenko A, Suzuki H, Rolland WB, Krafft PR, Zhang JH (2011) $\alpha 7$ nicotinic acetylcholine receptor agonist PNU-282987 attenuates early brain injury in a perforation model of subarachnoid hemorrhage in rats. *Stroke* 42(12):3530–3536
32. Cooke SF, Bliss TV (2006) Plasticity in the human central nervous system. *Brain* 129(Pt 7):1659–1673
33. Bliss TV, Collingridge GL (1993) A synaptic model of memory: long-term potentiation in the hippocampus. *Nature* 361(6407):31–39
34. Gutierrez-Venegas G, Torras-Ceballos A, Gomez-Mora JA, Fernandez-Rojas B (2017) Luteolin, quercetin, genistein and quercetin inhibit the effects of lipopolysaccharide obtained from *Porphyromonas gingivalis* in H9c2 cardiomyoblasts. *Cell Mol Biol Lett* 22:19
35. Kim SH, Shin KJ, Kim D, Kim YH, Han MS, Lee TG et al (2003) Luteolin inhibits the nuclear factor-kappa B transcriptional activity in Rat-1 fibroblasts. *Biochem Pharmacol* 66(6):955–963
36. Dajas F, Andres AC, Florencia A, Carolina E, Felicia RM (2013) Neuroprotective actions of flavones and flavonols: mechanisms and relationship to flavonoid structural features. *Cent Nerv Syst Agents Med Chem* 13(1):30–35
37. Chen CY, Peng WH, Tsai KD, Hsu SL (2007) Luteolin suppresses inflammation-associated gene expression by blocking NF-kappaB and AP-1 activation pathway in mouse alveolar macrophages. *Life Sci* 81(23–24):1602–1614
38. Norden DM, Muccigrosso MM, Godbout JP (2015) Microglial priming and enhanced reactivity to secondary insult in aging, and traumatic CNS injury, and neurodegenerative disease. *Neuropharmacology* 96(Pt A):29–41
39. Sofroniew MV, Vinters HV (2010) Astrocytes: biology and pathology. *Acta Neuropathol* 119(1):7–35
40. Pekny M, Johansson CB, Eliasson C, Stakeberg J, Wallen A, Perlmann T et al (1999) Abnormal reaction to central nervous system injury in mice lacking glial fibrillary acidic protein and vimentin. *J Cell Biol* 145(3):503–514
41. Gorina R, Font-Nieves M, Marquez-Kisinousky L, Santalucia T, Planas AM (2011) Astrocyte TLR4 activation induces a proinflammatory environment through the interplay between MyD88-dependent NFkappaB signaling, MAPK, and Jak1/Stat1 pathways. *Glia* 59(2):242–255
42. Zamanian JL, Xu L, Nouri N, Zhou L, Giffard RG et al (2012) Genomic analysis of reactive astrogliosis. *J Neurosci* 32(18):6391–6410
43. Paintlia AS, Paintlia MK, Singh AK, Singh I (2013) Modulation of Rho-Rock signaling pathway protects oligodendrocytes against cytokine toxicity via PPAR-alpha-dependent mechanism. *Glia* 61(9):1500–1517
44. Karve IP, Taylor JM, Crack PJ (2016) The contribution of astrocytes and microglia to traumatic brain injury. *Br J Pharmacol* 173(4):692–702
45. Brun A, Englund E (1986) A white matter disorder in dementia of the Alzheimer type: a pathoanatomical study. *Ann Neurol* 19(3):253–262
46. Thomalla G, Glauche V, Weiller C, Rother J (2005) Time course of wallerian degeneration after ischaemic stroke revealed by diffusion tensor imaging. *J Neurol Neurosurg Psychiatry* 76(2):266–268
47. Gu Y, Vorburgen RS, Gazes Y, Habeck CG, Stern Y, Luchsinger JA et al (2016) White matter integrity as a mediator in the relationship between dietary nutrients and cognition in the elderly. *Ann Neurol* 79(6):1014–1025